DMD Fast Forward. Published on April 1, 2009 as doi:10.1124/dmd.109.026898

Characterization of human hepatic and extrahepatic UDP-glucuronosyltransferase (UGTs) enzymes involved in the metabolism of classical cannabinoids

Anna Mazur, Cheryl F. Lichti, Paul L. Prather, Agnieszka K. Zielinska, Stacie M. Bratton, Anna Gallus-Zawada, Moshe Finel, Grover P. Miller, Anna Radominska-Pandya, Jeffery H. Moran

University of Arkansas for Medical Sciences Department of Biochemistry and Molecular Biology, University of Arkansas for Medical Sciences (AM, AZ, SB, AG-Z, GM, AR-P); Arkansas Department of Health, Arkansas Public Health Laboratory (CL, JM); Department of Internal Medicine, Washington University School of Medicine (CL); Department of Pharmacology and Toxicology, College of Medicine, University of Arkansas for Medical Sciences (PP); Centre for Drug Research (CDR), Faculty of Pharmacy, University of Helsinki, Finland (MF).

a) Running Title: **UDP-glucuronosyltransferase metabolism of cannabinoids**

b) Address correspondence to:

Jeffery H. Moran

Arkansas Public Health Laboratory

Arkansas Department of Health

201 South Monroe St.

Little Rock, AR 72205

(501) 661-2826 office

(501) 661-2972 fax

jeffery.moran@arkansas.gov

c) Important numbers

a. Text Pages: 12

b. Tables: 2

c. Figures: 6

d. References: 21

e. Words in Abstract: 248

f. Words in Introduction: 649

g. Words in Discussion: 603

d) Abbreviations: (-)-Δ^9-Tetrahydrocannabinol (Δ^9-THC), cytochrome P450 (P450), uridine diphosphate (UDP)-glucuronosyltransferases (UGTs); glucuronic acid (GlcUA); cannabinol (CBN), cannabidiol (CBD), (-)-Δ^8-Tetrahydrocannabinol (THC), (±)-11-hydroxy-Δ^9-THC (11-OH-THC), and (-)-11-nor-9-carboxy-Δ^9-THC (COOH-THC), Liquid chromatography-tandem mass spectrometry (LC-MS/MS); electrospray ionization (ESI), Morpine-6β-glucuronide (M6G)

Abstract

Tetrahydrocannabinol (Δ^9-THC), the primary psychoactive ingredient in marijuana, is subject to cytochrome P450 oxidation and subsequent UDP-glucuronosyltransferase (UGT) dependent glucuronidation. Many studies have shown that CYP2C9 and CYP3A4 are the primary enzymes responsible for these cytochrome P450 dependent oxidations, but little work has been done characterizing phase II metabolic pathways. This study tests the hypothesis that there are specific human UGTs responsible for classical cannabinoid metabolism. The activities of 12 human recombinant UGTs towards classical cannabinoids [cannabinol (CBN), cannabidiol (CBD), (-)-Δ^8-THC, (-)-Δ^9-THC, (±)-11-hydroxy-Δ^9-THC (11-OH-THC), and (-)-11-nor-9-carboxy-Δ^9-THC (COOH-THC)] were evaluated using HPLC-MS/MS and labeling assays. Despite activity by UGT1A1, -1A3, -1A8, -1A9, -1A10, and -2B7 toward CBN, CBD, 11-OH-THC, and COOH-THC, only selected UGTs demonstrate sufficient activity for further charaterization of steady-state kinetics. CBN was the most recognized substrate as evidenced by activities from hepatic UGT1A9 and extrahepatic UGT1A7, UGT1A8, and UGT1A10. These results may reflect the the introduction of an aromatic ring to Δ^9-THC, leading to favorable π stacking with phenylalanines in the UGT active site. Similarly, oxidation of Δ^9-THC to 11-OH-THC results in UGT1A9 and UGT1A10 activity toward the cannabinoid. Further oxidation to COOH-THC surprisingly leads to a loss in metabolism by UGT1A9 and UGT1A10, while creating a substrate recognized by UGT1A1 and UGT1A3. The resulting glucuronide of COOH-THC is the main metabolite found in urine, and thus these hepatic enzymes play a critical role in the metabolic clearance of cannabinoids. Taken together, glucuronidation of cannabinoids depends on upstream processing including enzymes such as CYP2C9 and CYP3A4.

Introduction

Cannabis sativa has been used both therapeutically and recreationally for centuries. Δ^9-Tetrahydrocannabinol (Δ^9-THC) is the main psychoactive ingredient in marijuana and mediates its effects primarily through activation of two G-protein coupled receptors, CB_1 and CB_2 (Howlett, 1995). Identified in 1990 (Matsuda et al., 1990), the human CB_1 receptor was found to be primarily localized in central and peripheral nervous tissue (Herkenham et al., 1990; Ishac et al., 1996). The CB_1 receptor has been identified as a therapeutic target in a variety of disease states, including obesity (Ravinet et al., 2002), alcohol dependence (Racz et al., 2003), pain (Iversen and Chapman, 2002) and Parkinson's disease (Brotchie, 2003). The second cannabinoid receptor, CB_2, cloned in 1993 (Munro et al., 1993) is found in immune tissues, most abundantly in the spleen and leukocytes (Galiegue et al., 1995). Selective CB_2 receptor ligands have potential therapeutic use as immune modulators for tumor suppression (Klein et al., 2003) and inflammation (Conti et al., 2002).

Cannabinoids are defined as compounds that are either structurally similar to THC or ligands that bind to cannabinoid receptors. While THC-related compounds are referred to as classical cannabinoids (Figure 1), ligands structurally distinct to THC also bind to CB1 and/or CB2 receptors and are classified as nonclassical cannabinoids, aminoalkylindoles and eicosanoids. The metabolism of the classical cannabinoids (the subject of this study) is very complex. For example, approximately 100 metabolites have thus far been identified for THC. The high lipid solubility of classical cannabinoids makes them good substrates for the cytochrome P450 mixed-function oxidases. Metabolism by CYP2C9 and CYP3A4 appears to account for most of the primary THC metabolites (Watanabe et al., 2007). For example, THC is hydroxylated at C11, at C8, and at all positions of the alkyl side-chain. C11 is the preferred hydroxylation site in man. In humans, CYP2C9 has been shown to catalyze the formation of the psychoactive 11-hydroxy metabolite of Δ^9-THC (Bornheim et al., 1992; Watanabe et al., 1995), and

CYP3A4 is responsible for hydroxylation at the 8β-position (Bornheim et al., 1992). Following the initial hydroxylation, many of the hydroxyl groups undergo further oxidation to primarily produce carboxylic groups at C11 and C5 (alkyl side chain). In contrast to phase I metabolism, very little is known about the phase II metabolism of classical cannabinoids. Phase II metabolites appear to be mainly conjugates of the phase I metabolites with glucuronic acid, catalyzed by the activity of UDP-glucuronosyltransferases (UGTs). For example, oxidation of the active metabolite Δ^9-THC-OH leads to the inactive metabolite 11-nor-9-carboxy-Δ^9-THC (COOH-THC). This modification of the cannabinoid also favors conjugation at the carboxyl position to form an *O*-esterglucuronide, which is the main metabolite found in urine (Yamamoto et al., 1987).

Although phase II metabolism is generally thought of as a pathway to inactivate drugs, it is well known that this pathway may also result in metabolic activation. For example, morpine-6β-glucuronide (M6G) is a phase II metabolite of morphine that appears to produce equivalent, long lasting analgesia and have an improved side effect profile relative to morphine (Wittwer and Kern, 2006). It has also been shown that acyl glucuronides of *all trans* retinoic acid and its derivatives exhibit significant biological activity. These compounds are less toxic than the parent compound yet retain the ability to drive cell growth, differentiation, and proliferation (Barua and Olson, 1987; Gallup et al., 1987; Janick-Buckner et al., 1991; Blaner and Olson, 1994). Therefore, it is possible that phase II metabolism of cannabinoids might also produce active compounds.

To better understand this metabolic pathway, identification of the human UGTs involved in metabolism of classical cannabinoids and product characterizations are required. Therefore, the purpose of the present study was to characterize potential glucuronidated products produced by human liver microsomes and 12 human recombinant UGTs in the presence of THC derivatives, cannabinol (CBN), cannabidiol (CBD), (-)-Δ^8-THC, (-)-Δ^9-THC, (±)-11-hydroxy-Δ^9-THC (11-OH-THC), and (-)-11-nor-9-

carboxy-Δ^9-THC (COOH-THC). Data show that both hepatic and extrahepatic UGTs selectively recognize certain cannabinoids for conjugation.

Materials and Methods

Materials

All chemicals used for this study were of at least reagent grade. Cannabinol (CBN), Cannabidiol (CBD), (-)-Δ^9-THC, (±)-11-hydroxy-Δ^9-THC, and (-)-11-nor-9-carboxy-Δ^9-THC were purchased from Cerilliant (Round Rock, TX). [^{14}C]UDP-GlcUA (325 mCi/mmol) was purchased from PerkinElmer Life Sciences (Boston, MA). Ethyl alcohol (95%) was purchased from AAPER (Shelbyville, KY). Unless otherwise specified, all other chemicals and reagents were of reagent grade and purchased from Sigma-Aldrich (St. Louis, MO).

Membrane fractions from baculovirus-infected insect cells expressing individual recombinant human UGTs were prepared as previously described (Kurkela et al., 2003; Kuuranne et al., 2003). Each enzyme tested in this study is known to be active toward substrates specific for that isoform. The expression level of individual recombinant UGTs was estimated by Western blot analyses using monoclonal antibodies (Tetra-His antibodies; Qiagen, Germany) against the His-tag that all of them carry (Kurkela et al., 2003). For activity comparison between individual UGTs, the enzyme level was normalized as previously described (Kuuranne et al., 2003).

Recombinant UGT Isoform Incubations

UGT activity was determined using [^{14}C]-UDP-GlcUA as the sugar donor for TLC analysis (Little et al., 2004) and unlabeled UDP-GlcUA for LC-MS/MS analysis. Briefly, UGT recombinant membrane protein (5 µg) was incubated in 100 µM Tris-HCl (pH 7.4)/5 mM $MgCl_2$/5 mM saccharolactone with 100 µM - 2000 µM substrate, in a total volume of 30 µl. Substrates were added in DMSO with a final concentration of 2%, and controls omitting substrates were run with each assay. Reactions were started by the addition of the appropriate UDP-GlcUA co-substrate (4 mM) and incubated at 37 °C for 90 min (screening) and 30 min (kinetics). Reactions were stopped by addition of 40 µl of ethanol.

TLC Analysis

TLC analysis of glucuronidation products form from [^{14}C]UDP-GlcUA were carried out as described previously (Radominska-Pyrek et al., 1987). In brief, aliquots (60 µl) of each incubation were applied to the preabsorbent layer of channeled silica gel TLC plates (Baker 250Si-PA (19C); VWR Scientific, Sugarland, TX) and glucuronidated products and unreacted substrate were separated by development in chloroform-methanol-glacial acetic acid-water (65:25:2:4, v/v). Radioactive compounds were localized on TLC plates by autoradiography for 3-4 days at -80 °C. Silica gel in areas corresponding to the glucuronide bands identified from autoradiograms and the corresponding areas from control lanes were scraped from the TLC plate into scintillation vials, and the radioactivity was measured by liquid scintillation counting (Packard TRI-CARB 2100TR, Perkin-Elmer). The results of these experiments were analyzed and apparent kinetic parameters were determined using Prism 4 software (GraphPad, San Diego, CA).

LC-MS/MS Analysis

Liquid chromatography-tandem mass spectrometry (LC-MS/MS) analyses for product confirmation were performed using an Agilent 1100 HPLC system (Santa Clara, CA) which was interfaced with an API 4000 triple quadrupole (MS/MS) mass spectrometer (Applied Biosystems, Foster City, CA). Instrument operation and data acquisition was controlled through the Analyst software package (Version 1.4.2, Applied Biosystems). The HPLC system consisted of an autosampler, a binary pump, and a column oven. Samples were loaded and resolved at a flow rate of 0.25 ml/min on a 4.0 x 50 mm phenyl column (YMC Phenyl 3 µm, Waters) maintained at 40 ºC. Mobile phases were 5 mM ammonium acetate (pH 6.5) in water (A) and acetonitrile (B). Compounds of interest were eluted using the following gradient: 50% B (0 min), linear gradient from 50% B to 60% B (0 to 2 min), linear gradient from 60% B to 90% B (2 to 3 min), linear gradient from 90% B to 100% B (3 to 4.1 min), 100% B (4.1

to 7.9 min), linear gradient from 100% B to 50% B (7.9 to 8 min), and 50% B (8.0 min. and after). Total run time, including a 2 min column pre-equilibration period, was 15 min. Injection volume was 5 μl. All MS/MS analyses were performed in negative ion mode by electrospray ionization (ESI) using a Turbo IonSpray source. Curtain, nebulizer, turbo, and collisionally-activated dissociation gases were 40 psig, 50 psig, 65 psig, 6 psig, respectively. Turbo heater temperature was 450 ºC, and ion spray voltage was -4500 V. Specific MS/MS experimental conditions are noted in Table 1.

Results

Cannabinoid Glucuronidation by Human Hepatic Microsomes and Recombinant UGTs

As an initial screen for glucuronidation activity toward cannabinoids, eight human recombinant UGT1A family UGTs expressed as His-tag proteins in baculovirus-infected Sf9 insect cells, four human recombinant UGT2B family over-expressed in HEK293 cells, and human liver microsomes were evaluated for their ability to glucuronidate 750 μM THC, CBN, CBD, (-)-Δ^9-THC, 11-OH-THC, or COOH-THC. (-)-Δ^9-THC did not appear to serve as a direct substrate for the tested human UGTs. This information indicates that native THC biotransformation is dependent on oxidations primarily catalyzed by CYP2C9 and CYP3A4 (Watanabe et al., 2007). UGT1A and 1B family isozymes showed variable responses in the presence of 11-OH-THC, COOH-THC, CBN, and CBD (Figure 2). The major product of CYP2C9 metabolism, 11-OH-THC, was specifically glucuronidated via UGT1A9 and 1A10. The highest activity towards COOH-THC was observed with UGT1A3, but HLM and UGT1A1 also showed a significant amount of activity towards this substrate. CBN, the product of THC degradation, was glucuronidated at high levels by UGT1A10 and to a lesser extent by UGT1A7, 1A9, and 2B7. Activity toward CBD was limited. HLM and UGT1A9, 2B7, and 2B17 all formed a minimal amount of a glucuronidated CBD product.

Product Confirmations/MS Spectral Interpretation

Even though some substrates did not appear to react during the initial screens (Figure 2), LC-MS/MS confirm that all the tested substrates served as substrates for human UGTs (Figure 3). Trace amounts of glucuronidated product was detected for all the substrates, but in some cases, where kinetic information could not be obtained, the physiological significance remains to be determined. MS2 chromatographs show predicted glucuronidated metabolites eluting within 2 min (Figure 3), and the corresponding MS2 spectra have a signals consistent with predicted glucuronidated metabolites (Figure 4 and 5). The

presence of *m/z* fragments of 313, 309, 343 and 313 in respective reactions suggest the loss of glucuronic acid. Since glucuronidated metabolites demonstrate a propensity to undergo in-source fragmentation during MS/MS analysis. Multiple reaction monitoring (MRM) experiments (data not shown) and neutral loss studies (data not shown) were designed to assess whether additional metabolites were formed but not identified during product ion scans. Neither study identified metabolites other than those observed in product ion scans (Figure 3). In particular, the presence of bis- and/or di-glucuronidated products was not detected. MRM studies showed a small degree of in-source fragmentation.

Definite regiochemical assignments can be made for the (-)-Δ^9-THC-(C1)-glucuronide, the CBN-(C1)-glucuronide, and the CBD-(C1)-glucuronide. C1 of (-)-Δ^9-THC and C1 of CBN are the only active sites which is recognized by UGTs (Figure 1). CBD contains two hydroxyl groups at the C1 and C5 positions (Figure 1). However, the C1 and C5 hydroxyl groups are identical due to free rotation about the bond at C6, and since no diglucuronidation was detected, there is only one possible glucuronide product. Although MS/MS data conclusively identified glucuronidated products for 11-OH-THC and COOH-THC, exact regiochemical assignments are complex because multiple reaction sites exist on these substrates and base product ions in mass spectra represent the loss of glucuronic acid. Additional information regarding regiochemistry of glucuronidation can be determined from fragments derived from the glucuronic acid moiety (Wen et al., 2007). Alcoholic and phenolic glucuronides are known to fragment by specific pathways, yielding ions of *m/z* 175 and 113 for phenolic glucuronides and of *m/z* 193, 175, and 113 for alcoholic glucuronides. MS2 spectrum of 11-OH-THC glucuronide (Figure 4) showing the absence *m/z* 193 indicates that the site of glucuronidation is on phenolic OH group. Likewise, the presence of the *m/z* 193 peak for COOH-THC (Figure 4) provides supporting evidence for glucuronidation of the carboylate group.

Steady-state Kinetics for Cannabinoid Glucuronidation by Recombinant UGTs

Based on our specific activity screen, we subjected selected UGTs to further catalytic studies to determine the respective steady-state parameters for cannabinoid glucuronidation (Figure 5 and Table 2). Despite MS characterizations confirming the glucuronide production for (-)-Δ^9-THC and CBD by UGT1A10 and UGT1A9, the sensitivity of TLC assessments was not adequate to obtain kinetic measurements. We were more successful with other enzymatic reactions. CBN undergoes glucuronidation by four different UGTs with a 17-fold variation in substrate binding. Hepatic UGT1A9 display the lowest K_m for CBN, while the extrahepatic enzymes, UGT1A7, UGT1A8, and UGT1A10, bound substrate more weakly based on higher K_m values. UGT1A9 and UGT1A10 also glucuronidate 11-OH-THC with affinities similar to those observed for CBN. Despite differences in structures, CBN and 11-OH-THC undergo glucuronidation at similar rates by UGT1A9. By contrast, UGT1A10 was 3-fold more effective at CBN conjugation than 11-OH-THC. Although hepatic UGT1A1 and UGT1A3 demonstrate the only measurable activity toward COOH-THC, these enzymes recognize the substrate more weakly than observed for the other reactions.

Discussion

Phase I oxidation and phase II conjugation of Δ^9-THC is generally accepted as important detoxification and excretion processes; however, the impact of these metabolic steps may be more complex than currently appreciated. This study begins characterizing specific human isozymes involved in glucuronidation of classical cannabinoids as well as characterizing products formed during these reactions. This is the first demonstration showing that several cannabinoids serve as substrates for specific human UGTs and HLM and that classical cannabinoid metabolism appears to be tissue specific.

LC-MS/MS analysis of product mixtures confirms that glucuronide conjugation does indeed occur for all classical cannabinoids tested. Product ion scans of the desired mono-glucuronides provide MS/MS spectra for species with appropriate mass and in most cases allow for specific regiochemistry assignments. Δ^9-THC, CBN, and CBD are all glucuronidated at the C1 position. However, the C5 position is equivalent to C1 in CBD because there is free rotation about the chemical bond localized at the C6 position. Regiochemical assignments for 11-OH-THC and COOH-THC are not as straightforward, because these substrates contain multiple reaction sites that can give rise to different glucuronides. Reactions can occur on the carboxyl terminus of COOH-THC, on the allylic side chain of 11-OH-THC or on the phenolic group which is located in both COOH-THC and 11-OH-THC. Structure comparisons as well as substrate recognition studies suggest that glucuronidation is occurring on carboxyl terminus and on the phenolic hydroxyl group. Analyses of mass spectrum are also consistent with these conclusions (Wen et al., 2007).

The extent of cannabinoid glucuronidation ultimately depends upon structural differences among the compounds. Despite the presence of a hydroxyl group at C1 position, Δ^9-THC is not readily recognized as substrate for glucuronidation unless transformed into CBN. This plant-catalyzed process introduces an aromatic ring into the structure of the molecule and subsequently results in the metabolism of this

cannabinoid by hepatic UGT1A9 and the extrahepatic UGTs, UGT1A7, UGT1A8, and UGT1A10. The recognition of CBN by these UGTs likely involves π stacking with active site phenylalanines, such as those identified in binding motif for UGT1A10 (Xiong et al., 2006). These enzyme-substrate contacts would favor binding and possibly properly orient the molecule for conjugation. The relative impact of substrate recognition is not uniform among the UGTs. For example, UGT1A9 displays the highest affinity for CBN while UGT1A10 has the lowest.

CYP2C9 oxidation of Δ^9-THC generates 11-OH-THC, a substrate preferentially metabolized by UGT1A9 but also recognized by UGT1A10. It appears that the additional hydroxyl function group to Δ^9-THC provides an alternate site for conjugation and/or alters the binding mode for the cannabinoid to favor UGT catalysis. Further oxidation of 11-OH-THC to COOH-THC surprisingly leads to a loss in metabolism by UGT1A9 and UGT1A10, while creating a substrate recognized by hepatic UGT1A1 and UGT1A3. These UGTs must be better suited to tolerate the introduction of a full negative charge to the cannabinoid. The resulting *O*-esterglucuronide of COOH-THC is the main metabolite found in urine (Yamamoto et al., 1987), and thus these hepatic enzymes play a critical role in the metabolic clearance of cannabinoids. Taken together, phase II metabolism of cannabinoids depends on upstream processing including by enzymes such as CYP2C9 and CYP3A4 (Watanabe et al., 2007).

This report characterizes human UGTs associated with classical cannabinoids metabolism and provides information which will be necessary to fully explore the importance of this metabolic pathway. This study shows that UGT activity is controlled through specific P450 oxidations as well as specific enzyme-substrate mechanisms. Future studies assessing the biological activity of novel metabolites presented in this study may provide insight in developing better pain treatment options as well as help our understanding of drug dependence.

Acknowledgements

The authors would like to thank Mika Kurkela for his technical review as well as Richard Bonner, Benjamin Jefferson, Suzanne Owen and Johanna Mosorin for their technical assistance.

References

Barua AB and Olson JA (1987) Chemical synthesis and growth-promoting activity of all-trans-retinyl beta-D-glucuronide. *Biochemical Journal* **244:**231-234.

Blaner WS and Olson JA (1994) Retinol and retinoic acid metabolism., in: *The Retinoids. Biology, Chemistry, and Medicine.* (Sporn MB, Roberts AB and Goodman DS eds), pp 229-255, Raven Press, New York.

Brotchie JM (2003) CB1 cannabinoid receptor signalling in Parkinson's disease. *Current Opinion in Pharmacology* **3:**54-61.

Galiegue S, Mary S, Marchand J, Dussossoy D, Carriere D, Carayon P, Bouaboula M, Shire D, Le Fur G and Casellas P (1995) Expression of central and peripheral cannabinoid receptors in human immune tissues and leukocyte subpopulations. *European Journal of Biochemistry* **232:**54-61.

Gallup JM, Barua AB, Furr HC and Olson JA (1987) Effects of retinoid beta-glucuronides and N-retinoyl amines on the differentiation of HL-60 cells in vitro. *Proc Soc Exp Biol Med* **186:**269-274.

Howlett AC (1995) Pharmacology of cannabinoid receptors. *Annual Review of Pharmacology and Toxicology* **35:**607-634.

Iversen L and Chapman V (2002) Cannabinoids: a real prospect for pain relief. *Current Opinion in Pharmacology* **2:**50-55.

Janick-Buckner D, Barua AB and Olson JA (1991) Induction of HL-60 cell differentiation by water-soluble and nitrogen-containing conjugates of retinoic acid and retinol. *Faseb J* **5:**320-325.

Klein T, Newton C, Larsen K, Lu L, Perkins I, Liang N and Friedman H (2003) The cannabinoid system and immune modulation. *Journal of Leukocyte Biology* **74:**486-496.

Kurkela M, Garcia-Horsman JA, Luukkanen L, Morsky S, Taskinen J, Baumann M, Kostiainen R, Hirvonen J and Finel M (2003) Expression and characterization of recombinant human UDP-glucuronosyltransferases (UGTs). UGT1A9 is more resistant to detergent inhibition than other UGTs and was purified as an active dimeric enzyme. *J Biol Chem* **278:**3536-3544.

Kuuranne T, Kurkela M, Thevis M, Schanzer W, Finel M and Kostiainen R (2003) Glucuronidation of anabolic androgenic steroids by recombinant human UDP-glucuronosyltransferases. *Drug Metab Dispos* **31:**1117-1124.

Little JM, Kurkela M, Sonka J, Jantti S, Ketola R, Bratton S, Finel M and Radominska-Pandya A (2004) Glucuronidation of oxidized fatty acids and prostaglandins B1 and E2 by human hepatic and recombinant UDP-glucuronosyltransferases. *J Lipid Res* **45:**1694-1703.

Matsuda L, Lolait S, Brownstein M, Young A and Bonner T (1990) Structure of a cannabinoid receptor and functional expression of the cloned cDNA. *Nature* **346:**561-564.

Munro S, Thomas K and Abu-Shaar M (1993) Molecular characterization of a peripheral receptor for cannabinoids. *Nature* **365:**61-65.

Racz I, Bilkei-Gorzo A, Toth Z, Michel K, Palkovits M and Zimmer A (2003) A critical role for the cannabinoid CB1 receptors in alcohol dependence and stress-stimulated ethanol drinking. *Journal of Neuroscience* **23:**2453-2458.

Radominska-Pyrek A, Zimniak P, Irshaid YM, Lester R, Tephly TR and St Pyrek J (1987) Glucuronidation of 6 alpha-hydroxy bile acids by human liver microsomes. *J Clin Invest* **80:**234-241.

Ravinet T, Arnone M, Delgorge C, Gonalons N, Keane P, Maffrand J and Soubrie P (2002) Anti-obesity effect of SR141716, a CB1 receptor antagonist, in diet induced obese mice. *American Journal of Physiological Regulatory Integrative Comparative Physiology* **284:**345-353.

Wen Z, Tallman MN, Ali SY and Smith PC (2007) UDP-glucuronosyltransferase 1A1 is the principal enzyme responsible for etoposide glucuronidation in human liver and intestinal microsomes: structural characterization of phenolic and alcoholic glucuronides of etoposide and estimation of enzyme kinetics. *Drug Metab Dispos* **35:**371-380.

Wittwer E and Kern SE (2006) Role of morphine's metabolites in analgesia: concepts and controversies. *American Association of Pharmaceutical Scientists* **8:**E348-352.

Xiong Y, Bernardi D, Bratton S, Ward MD, Battaglia E, Finel M, Drake RR and Radominska-Pandya A (2006) Phenylalanine 90 and 93 are localized within the phenol binding site of human UDP-glucuronosyltransferase 1A10 as determined by photoaffinity labeling, mass spectrometry, and site-directed mutagenesis. *Biochemistry* **45:**2322-2332.

Yamamoto I, Watanabe K, Kuzuoka K, Narimatsu S and Yoshimura H (1987) The pharmacological activity of cannabinol and its major metabolite, 11-hydroxycannabinol. *Chemical and Pharmaceutical Bulletin* **35:**2144-2147.

Footnotes

This work was supported by the National Institutes of Health [Grant NIH-DK60109 and NIH-GM075893], by the Centers for Disease Control [Cooperative Agreement U90/CCU616974-07], the Association of Public Health Laboratories [EH Training fellowship], and the Academy of Finland [Project 210933].

Legends for Figures

Figure 1 Structures of Cannabinoids under investigation.

Figure 2 Glucuronidation Activity Screening. Selected recombinant UGT isoforms and human liver microsomes were screened for activity toward CBN, 11-OH-THC, COOH-THC, and CBD. Glucuronidation activities were measured by incubating microsomal protein (5 µg recombinant UGT; 50 µg HL) with substrate (500 µM) and UDP-GlcUA (4 mM). All reactions were normalized as described in *Materials and Methods*.

Figure 3 RP-HPLC chromatographs of glucuronidated-product ion experiments. Tracings represent organic-soluble metabolites generated during incubation of recombinant protein with UDP-glucuronic acid (4 mM) and 750 µM of each substrate (A) CBN, B) CBD and C) 11-OH-THC, and D) COOH-THC) Each substrate was incubated individually for 180 min. Control reactions omitted the respective substrate. MS/MS data were obtained in negative ion mode, as described in *Materials and Methods* .

Figure 4 MS/MS spectra of the glucuronides of (A) Δ^9-THC, (B) CBN, (C) 11-OH-THC, (D) CBD, and (E) COOH-THC. Spectra are representative of the glucuronidated products shown in Figure 3. Data were obtained in negative ion mode as described in *Materials and Methods*.

Figure 5 Proposed MS/MS fragmentation pathways for (A) Δ^9-THC, (B) CBN, (C) 11-OH-THC, (D) CBD, and (E) COOH-THC glucuronides.

Figure 6 Steady-state glucuronidation of A) CBN, B) 11-OH-THC and C) COOH-THC with selected recombinant UGT isoforms. Glucuronidation activities of recombinant proteins were measured by incubating membrane fractions containing recombinant UGT1A10 (5 µg) with increasing concentrations (shown in the figure) of substrate at a constant concentration of UDP-GlcUA (4 mM).

Curve fits and kinetic constants were determined using GraphPad Prism 4 software and the resulting parameters are included in Table 2.

Table 1. MS/MS Experimental Conditions for Product Ion, Multiple Reaction Monitoring (MRM), and Neutral Loss Studies

		Analyte	Q1 (m/z)	Q3 (m/z)	CE[a] (V)	EP[b] (V)	DP[c] (V)	CXP[d] (V)
Product Ion	1	CBN-Gluc	485.1	50 - 525	-20 to -35	-10	-50 to -70	-9 to -15 (2 sec)
	2	THC-O-Gluc	505.3	50 - 510	-30 to -40	-10	-50 to -70	-9
	3	THC-CO-O-Gluc	519.3	50 - 525	-30 to -40	-10	-50 to -70	-9
MRM	1	CBN	309.3	171.1	-40	-10	-89	-3
			309.3	279.2	-42	-10	-91	-7
	2	Δ9-THC and CBD	313.3	191.2	-38	-10	-87	-3
			313.3	245.3	-36	-10	-82	-5
	3	THC-OH	329.3	268.3	-38	-10	-69	-6
			329.3	311.2	-25	-10	-65	-8
	4	THC-COOH	343.2	245.2	-40	-10	-82	-5
			343.2	299.3	-29	-10	-75	-7
	5	CBN-Glucuronide	485.1	113.2	-29	-10	-61	-8
			485.1	309.2	-27	-10	-76	-8
	6	Δ^9-THC-Gluc and CBD-Gluc	489.3	313.1	-35	-10	-61	-8
			489.3	374.9	-30	-10	-76	-9
	7	THC-OH Gluc	505.3	311.2	-44	-10	-56	-8
			505.3	329.2	-31	-10	-59	-8
	8	THC-COO-Gluc	519.3	193.2	-25	-10	-47	-8
			519.3	343.3	-33	-10	-36	-9
Neutral Loss	1	Loss of glucuronic acid	loss of 176 (400 - 800 amu)		-20 to -35	-10	-50 to -80	-9 to -15 (2 sec)

[a]Collision Energy, [b]Entrance Potential, [c]Declustering Potential, [d]Collision Cell Exit Potential

Table 2. Steady-state parameters for glucuronidation of CBN, 11-OH-THC and COOH-THC by UGT isoforms.[a]

Substrate	*UGT isoform*[b]	V_{max} *(nmol/mg protein/min)*	K_m *(μM)*	V_{max}/K_m *(μl/mg protein/min)*
CBN	UGT1A7	0.24 ± 0.01	19 ± 3.9	12.6
	UGT1A8	0.49 ± 0.03	44 ± 8.1	11.1
	UGT1A9	0.10 ± 0.01	3.4 ± 1.3	29.4
	UGT1A10	0.91 ± 0.05	59 ± 10	15.4
11-OH-THC	UGT1A9	0.14 ± 0.01	7.3 ± 1.9	19.2
	UGT1A10	0.33 ± 0.03	72 ± 19	4.58
COOH-THC	UGT1A1	0.22 ± 0.02	170 ± 37	1.29
	UGT1A3	0.68 ± 0.06	68 ± 17	10.0

[a]Parameters determined from the fit of initial velocities to a Michaelis-Menten kinetic scheme using the software GraphPad Prism. [b]All reactions were normalized as described in *Materials and Methods*.

Figure 1.

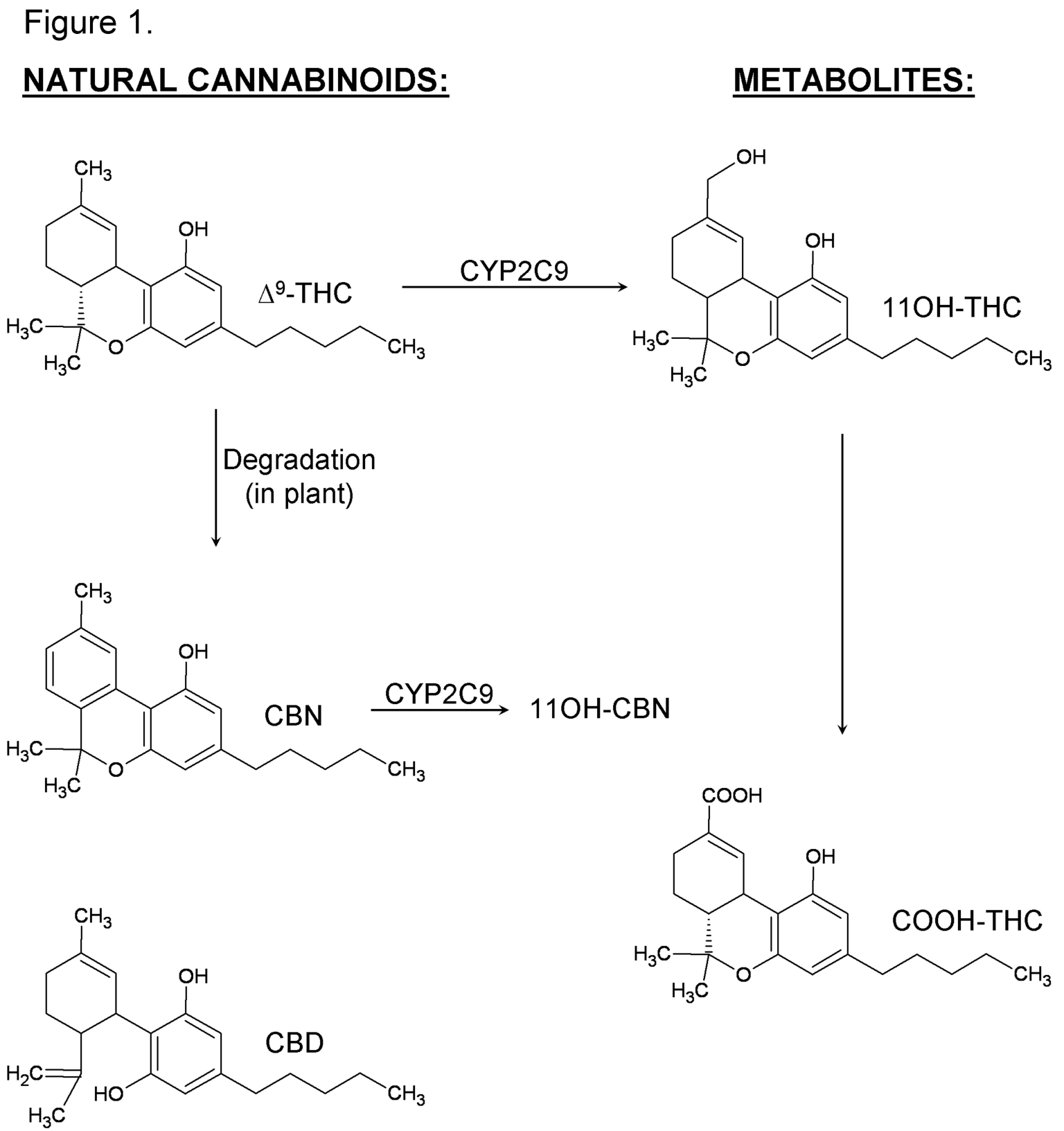
NATURAL CANNABINOIDS:
METABOLITES:
CH3
OH
Δ9-THC
H3C
H3C
O
CH3
CYP2C9
OH
OH
11OH-THC
Degradation
(in plant)
CBN
CYP2C9
11OH-CBN
COOH
OH
COOH-THC
CBD
H2C
HO

Figure 2.

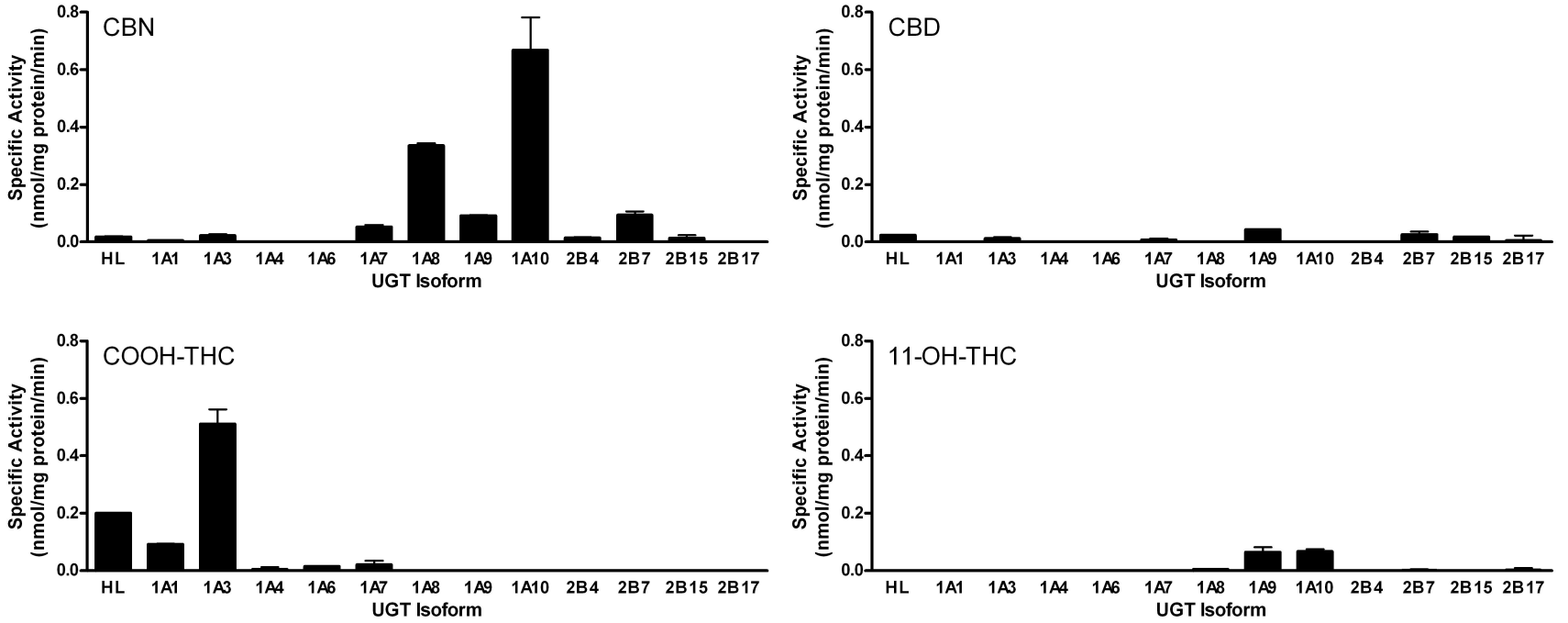
CBN
CBD
COOH-THC
11-OH-THC
Specific Activity (nmol/mg protein/min)
0.0
0.2
0.4
0.6
0.8
HL
1A1
1A3
1A4
1A6
1A7
1A8
1A9
1A10
2B4
2B7
2B15
2B17
UGT Isoform

Figure 3

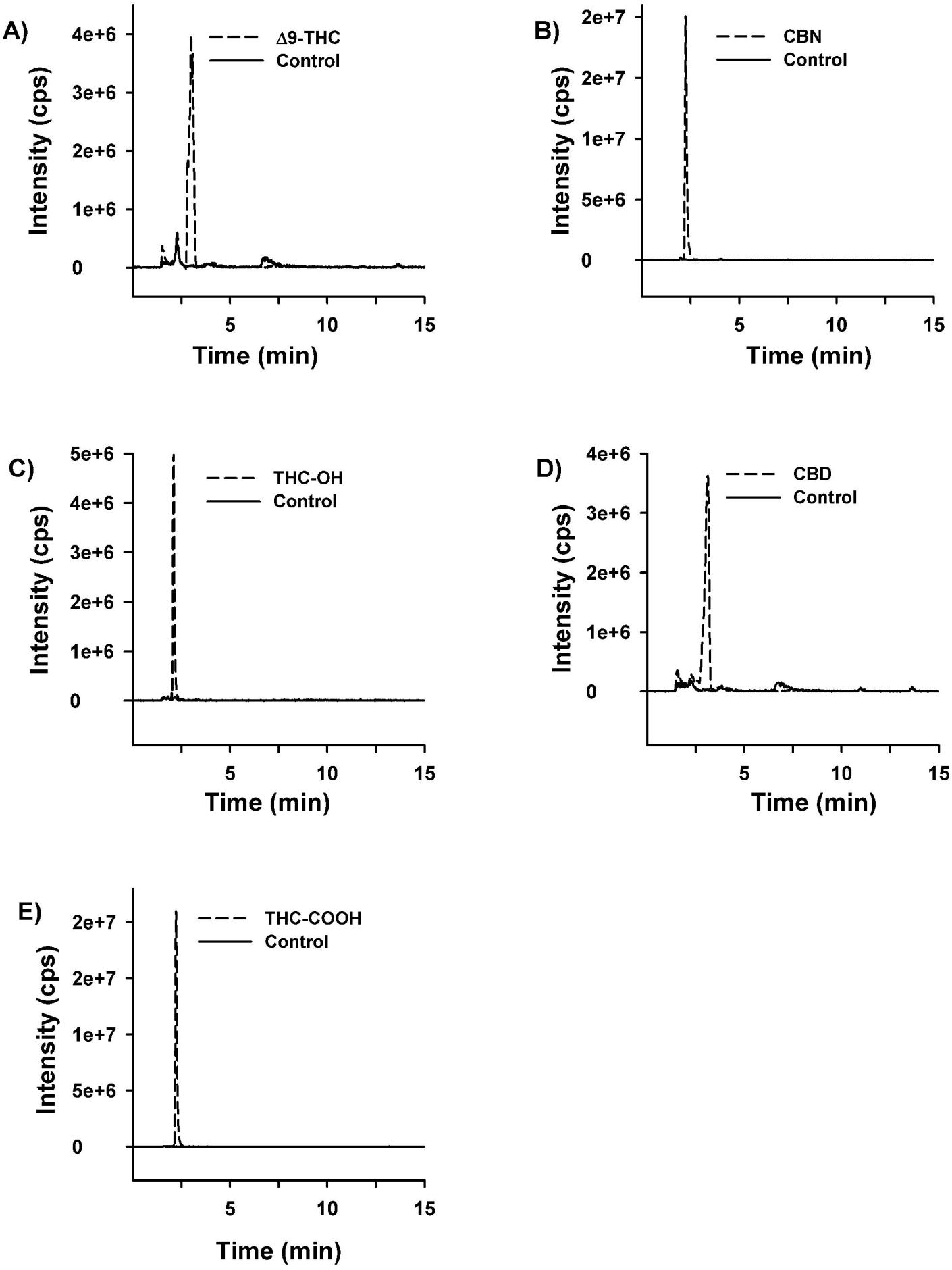
A)
Δ9-THC
Control
Intensity (cps)
4e+6
3e+6
2e+6
1e+6
0
5
10
15
Time (min)
B)
CBN
Control
Intensity (cps)
2e+7
2e+7
1e+7
5e+6
0
5
10
15
Time (min)
C)
THC-OH
Control
Intensity (cps)
5e+6
4e+6
3e+6
2e+6
1e+6
0
5
10
15
Time (min)
D)
CBD
Control
Intensity (cps)
4e+6
3e+6
2e+6
1e+6
0
5
10
15
Time (min)
E)
THC-COOH
Control
Intensity (cps)
2e+7
2e+7
1e+7
5e+6
0
5
10
15
Time (min)

Figure 4

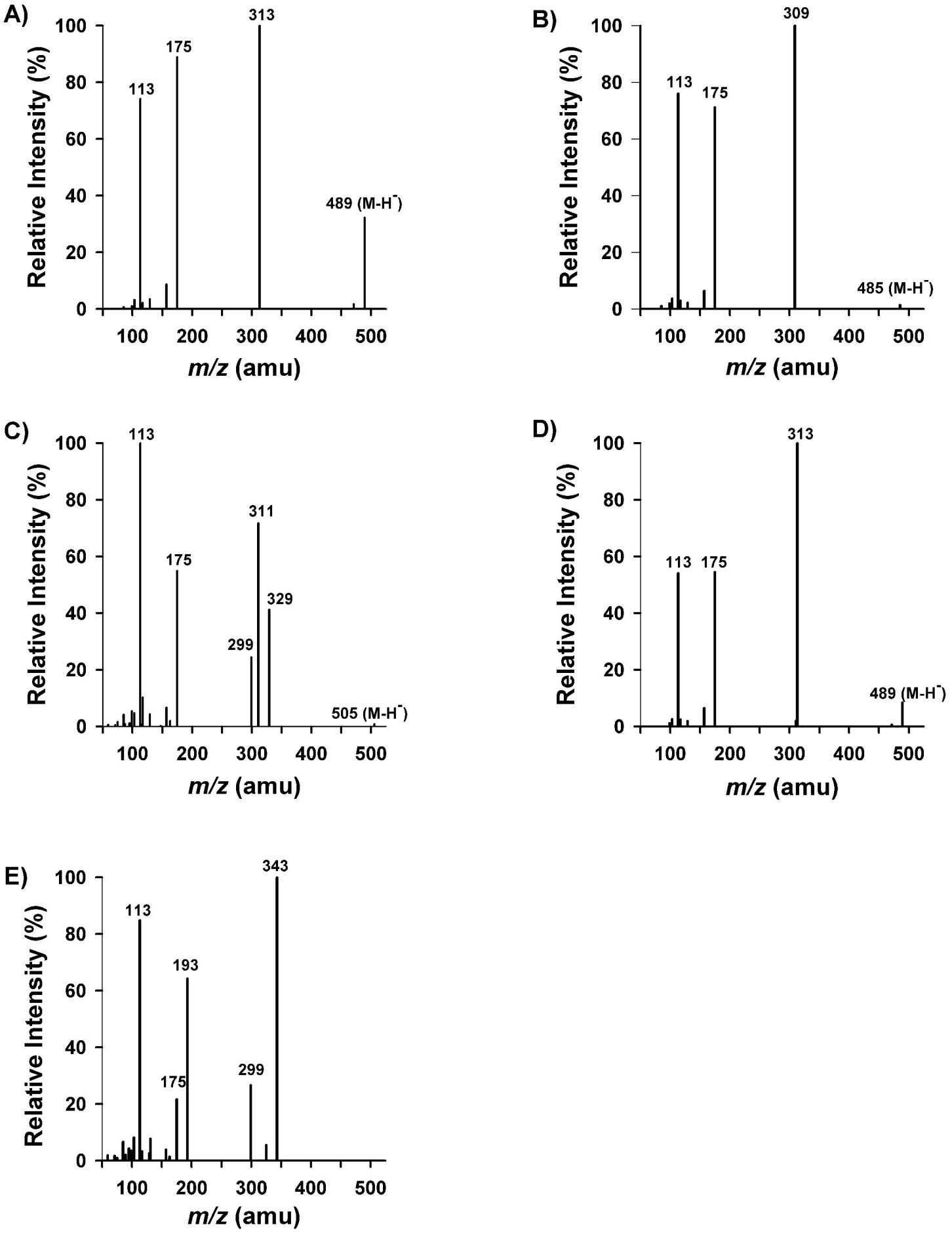
A)
Relative Intensity (%)
m/z (amu)
313
175
113
489 (M-H-)
B)
309
113
175
485 (M-H-)
C)
113
311
175
329
299
505 (M-H-)
D)
313
113
175
489 (M-H-)
E)
343
113
193
175
299

Figure 5

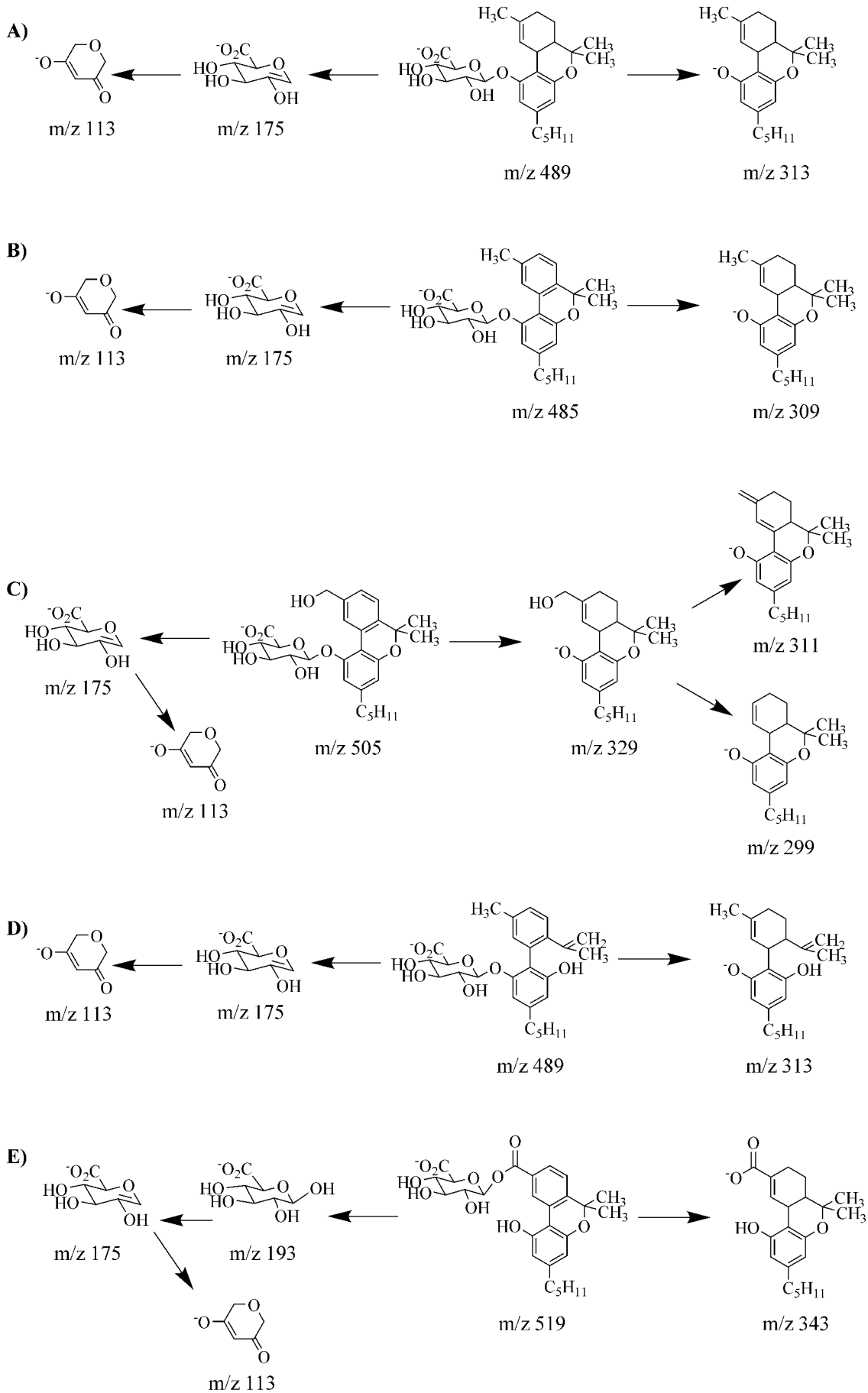
A)
m/z 113
m/z 175
m/z 489
m/z 313
B)
m/z 113
m/z 175
m/z 485
m/z 309
C)
m/z 175
m/z 113
m/z 505
m/z 329
m/z 311
m/z 299
D)
m/z 113
m/z 175
m/z 489
m/z 313
E)
m/z 175
m/z 193
m/z 113
m/z 519
m/z 343

Figure 6.

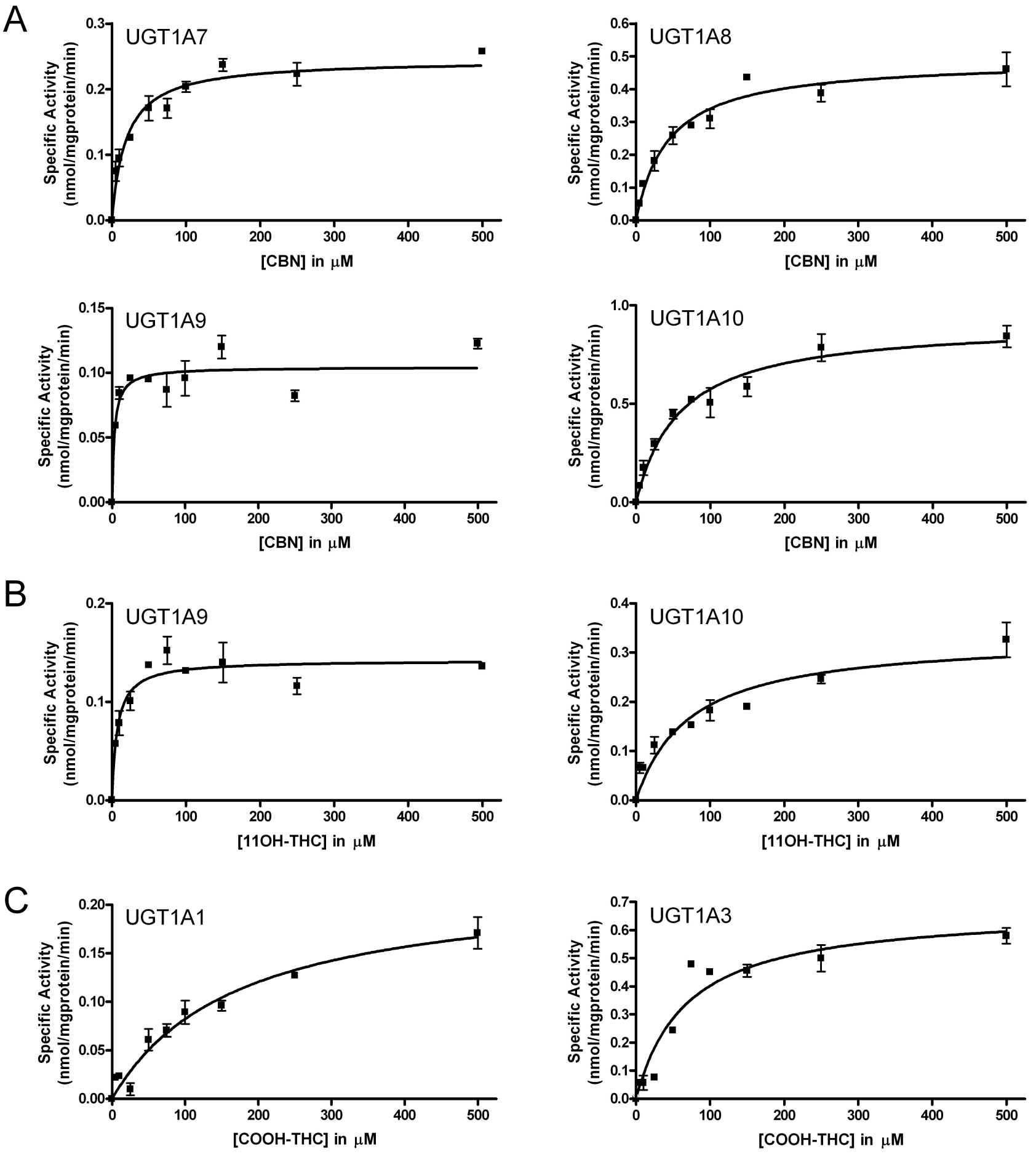
A
UGT1A7
Specific Activity (nmol/mgprotein/min)
[CBN] in μM
UGT1A8
Specific Activity (nmol/mgprotein/min)
[CBN] in μM
UGT1A9
Specific Activity (nmol/mgprotein/min)
[CBN] in μM
UGT1A10
Specific Activity (nmol/mgprotein/min)
[CBN] in μM
B
UGT1A9
Specific Activity (nmol/mgprotein/min)
[11OH-THC] in μM
UGT1A10
Specific Activity (nmol/mgprotein/min)
[11OH-THC] in μM
C
UGT1A1
Specific Activity (nmol/mgprotein/min)
[COOH-THC] in μM
UGT1A3
Specific Activity (nmol/mgprotein/min)
[COOH-THC] in μM